Foreseeing private car transfer between urban regions with multiple graph-based generative adversarial networks

Chenxi Liu[1] · Zhu Xiao[1] · Dong Wang[1] · Minhao Cheng[2] · Hongyang Chen[3] · Jiawei Cai[1]

Abstract

Private car transfer indicates that people drive private cars and travel between urban regions to perform daily activities. Foreseeing private car transfer between urban regions can facilitate a broad scope of applications ranging from route planning, hot region discovery to urban computing. However, three challenges remain. *i*) Private car transfer between regions is affected by multiple spatio-temporal correlations. *ii*) Transfer records are highly sparse and imbalanced. *iii*) Modeling the stay duration of private cars. In this paper, we model private cars' travel in urban regions as the spatio-temporal graph and formulate private car transfer foreseeing as the time-evolving adjacency matrix prediction of the graph. To specify, we propose MG-GAN (**M**ultiple **G**raph-based **G**enerative **A**dversarial **N**etwork) to predict private car transfer. For one thing, we design multi-graph dense convolutions with gated recurrent networks as the generative network to capture multiple spatio-temporal correlations. For another, the attentive multi-graph convolutional network is designed as the discriminative network to learn the stay duration correlations of private cars in each region. The iterative adversarial processes between generating and discriminating networks enhance the MG-GAN's ability to tackle the sparse data problem. Besides, a topic clustering algorithm based on multi-source data fusion is proposed to balance the fused data. Extensive experiments on the real-world private car and taxi trip datasets demonstrate that MG-GAN performs better than the state-of-the-art baselines.

Keywords Private car · Transfer flow · Mulitple graph · Generative adversarial networks · Spatio-temporal prediction

  🦦 Springer

1 Introduction

1.1 Background and motivation

Private car transfer indicates that people drive their private cars to travel between urban regions to perform daily activities and fulfill travel needs. In particular, private cars contribute to the essential part of urban traffic (taking China as an example, nearly 86.6% of the urban automobiles are private cars) [35]. People usually drive private cars transferring between residential regions and the workplaces on weekday mornings, the shopping regions on weekends [4], thereby generating transfer flows at the corresponding periods. Foreseeing private car transfer benefits understanding human mobility and their travel patterns. For example, city managers can foresee the private car flows in every region and know the direction of these flows, that is, where the origin and destination regions are. Furthermore, the predicted transfer information will significantly assist the analysis of how a region affects others, which is of utmost essential for urban transportation development, ranging from route planning, hot region discovery to urban computing [2, 10, 21].

Over the years, fewer works have focused on private car transfer between urban regions, and the most similar task is OD (Origin-Destination) transfer prediction. Many scholars construct the task based on urban traffic data, e.g., taxi, shared bicycle, and subway data [23, 32]. In [8], authors regarded OD matrix as image data and proposed a multi-scale convolutional recurrent network for predicting taxi flows between OD pairs. However, they considered the divided regions as a whole image, ignoring the non-European correlations between regions. To preserve the non-European correlations between regions, some works modeled urban regions based on the graph [29]. Moreira et al. estimated time-evolving OD matrix using high-speed GPS data [22]. Their grid-based region-division method is contrary to the irregularity of the original urban regions. Some works divided the city into irregular regions [1]. In [11], the authors divided the city into irregular regions according to the road network. Nevertheless, they did not make full use of irregular regions' temporal similarity and semantic correlation.

1.2 Challenges

Recent advances in deep neural networks can be applied to predict the private car transfer [11, 16, 29]. However, it is not straightforward to apply these methods to private car transfer prediction between urban regions because of the following challenges. *i)* Multiple spatio-temporal correlations. Private car transfer between urban regions is affected by several factors, such as travel distance, region similarity, weather, and date. To effectively predict private car transfer, it is required to model these factors collaboratively. However, the spatio-temporal correlations among multiple factors in private car transfer are not fully explored. How to comprehensively measure the region similarities to infer the regions' attractiveness to private cars at different periods is still a problem. *ii)* Imbalanced and sparse transfer records. Private car transfer records are often skewed in the spatial and temporal dimensions. To specify, private car users usually go to certain preferred regions. Accordingly, some regions have frequent inflows, while others have a few. This phenomenon results in the spatial imbalance of private car transfer records. In the temporal dimension, when private car users drive to a specific region, they will stop the car and stay in the region for a certain duration enjoying themselves or doing their businesses. Such stay duration leads to discontinuous and sparse transfer records. *iii)* Modeling the stay duration of private cars. The existing works apply sequence methods to extract the sequential temporal correlations.

Nevertheless, in practical applications, in addition to the sequential temporal correlations, the stay duration correlations provide a crucial attribute reflecting the regularity of private car transfer. For instance, after the private car is transferred to a region, it will stay in this region for a while [13]. The longer a private car stays in one region, the more attractive the region is to the car's owner. The stay duration of private cars is closely related to the attractiveness of regions, which in turn affects the private car transfer, they are constantly influencing each other. Existing works only model sequential time series for all regions, while the stay duration characteristics in each region are often overlooked.

1.3 Solution

In this paper, we develop the MG-GAN (**M**ultiple **G**raph-based **G**enerative **A**dversarial **N**etwork) so as to effectively address the above-mentioned challenges. First, we collect and fuse multi-source data, including private car trips, AOI (area-of-interest), POI (point-of-interest), weather, and date. Second, we propose a topic clustering algorithm based on multi-source data fusion to identify urban functional regions. This algorithm solves the problem of data imbalance since AOIs with close distances are clustered into functional regions. Third, we model private cars' travel in functional regions as multiple spatio-temporal graph. Fourth, we formulate the private car transfer prediction as to the time-evolving adjacency matrix prediction of the graph. Based on this, we propose the MG-GAN, which consists of a generative network and a discriminative network. For one thing, the multi-graph dense convolutions with the gated recurrent network are proposed as the generative network. Precisely, the multi-graph dense convolutions can capture regions' spatial correlations in each period. The learned graph representations are fed into dense gated recurrent units to capture the graph's temporal correlations with successive periods. For another, inspired by the constant interactions between the stay duration and the region attractiveness, we design the attentive network with multi-graph convolution as the discriminative network to compete with the generative network. The iterative adversarial processes between generating and discriminating networks enhance the MG-GAN's ability to tackle the sparse data problem. Meanwhile, the attentive multi-graph convolution network is used to learn the stay duration correlations of private cars in each region. Extensive experiments on real-world private car trip datasets demonstrate that MG-GAN achieves better performances compared to the baselines.

1.4 Contributions

The main contributions of this paper are outlined as follows:

– We propose MG-GAN, a deep adversarial model to foresee private car transfer between urban regions effectively. MG-GAN consists of a generative network and a discriminative network. The multi-graph dense convolutions with gated recurrent networks as the generative network to capture multiple spatio-temporal correlations.
– We design the attentive network with multi-graph convolution as the discriminative network to learn the stay duration correlations of private cars in each region. The iterative adversarial processes between generating and discriminating networks enhance the MG-GAN's ability to tackle the sparse data problem. In addition, a topic clustering algorithm based on multi-source data fusion is proposed to balance the fused data.

–   We conduct extensive experiments on real-world private car and taxi trip datasets. The experimental results demonstrate that MG-GAN achieves better performances than baselines.

The remainder of this paper is organized as follows. Section 2 summarizes related works. Section 3 presents the definitions and problem statement. Section 4 details the methodological framework. Section 5 introduces the experiments and further analysis. Finally, Section 6 concludes the paper.

2 Related work

2.1 Origin-destination transfer prediction

OD transfer prediction in region level aims to estimate interactions, such as crowd flows [10], travel times [17], or stochastic speeds [25], between origin and destination regions. Many scholars construct the task based on urban traffic data, e.g., taxi, shared bicycle, and subway data [23]. In [8], authors regarded OD matrix as image data. They proposed a multi-scale convolutional recurrent network for predicting taxi flows between OD pairs. Zhang et al. proposed a three-stream fully CNN (convolutional neural network) to forecast the edge flows between vertices in spatio-temporal networks [32]. However, they regarded the divided regions as a whole image, ignoring the non-European correlations between regions. To preserve the non-European correlations between regions, some works modeled urban regions based on the graph. Moreira et al. estimated time-evolving OD matrix using high-speed GPS data [22]. Authors in [29] used GCN (graph convolutional network) and RNN (recurrent neural network) to predict the OD matrix. However, their grid-based region-division method is contrary to the irregularity of the original urban regions. Some works divided the city into irregular regions [1]. In [11], the authors divided the city into irregular regions according to the road network. Nevertheless, they did not make full use of irregular regions' semantic information. Compared to these works, we divide the city into urban functional regions with semantic information and model the non-European relationship between regions through graph-based networks.

2.2 Graph-based neural networks for spatio-temporal prediction

Since the graph-based neural network can capture the non-Euclidean correlations of traffic data, most scholars use GCN integrated with RNNs, CNNs, or attention to conduct the spatio-temporal prediction task [7]. Chai et al. utilized a multi-graph convolutional network to predict station-level traffic flows, with the recurrent neural network as the encoder-decoder [6]. However, they were unable to capture the semantic correlations between bicycle stations. Geng et al. employed multi-graph convolution and contextual gated RNN to predict ride-hailing demand [9]. Luo et al. performed an attention multi-graph convolutional sequence-to-sequence model for station-level flow prediction [25]. These works did not fully consider the temporal similarity of different vertices in the graph, making it difficult to model spatio-temporal correlations jointly. Furthermore, these methods can not be directly applied to solve imbalanced and sparse data on the graph structure. In this study, we construct temporal similarity graphs to model spatio-temporal correlations jointly. Besides, we solve imbalanced data problems through the proposed clustering algorithm and solve sparse data by designing densely connected graph neural networks.

Recently, GAN-based techniques have been shown to be promising for spatio-temporal prediction [34]. Lei et al. proposed GCN-GAN, which combined GCN, long short-term memory (LSTM), and GAN to predict temporal links in graphs [16]. Yang et al. designed an attentive GCN model for temporal link prediction using GAN [30]. The attentive GCN allows assigning different importance to the vertices to learn the dynamic network's spatial features. The above two state-of-the-art works are more related to ours. However, unlike these, our work focuses on real-world cases and reflects the dynamic interactions between urban functional regions from private cars' perspectives. Instead of merely applying GCN for adversarial learning, we design multi-graph dense convolutions with gated recurrent networks as the generative network. Besides, we create the discriminative network based on the private cars' stay duration to conduct adversarial learning with the generation network.

3 Definitions and problem statements

In this section, we introduce essential definitions and problem statements, which will be used throughout this study. Further, we summarize the main notations used in this article in Table 1.

Definition 1 Urban Region. We use three parallel division ways to model city's geological information: the grid, AOI and functional region (FR). **(1) Grid.** We build up a city-wide geographical grid region set **gr**, each equal-sized grid in **gr** is called a region $gr_{[i, j]}$, where $[i, j]$ denotes the center coordinates of a grid. **(2) AOI.** City could be represented by urban AOI region set **ar**, each AOI is denoted by ar_{id}, the id is the unique identifier of AOI. **(3)**

Table 1 Main notations and descriptions

Notation	Description
$\mathcal{G}$	Spatio-temporal graph
$\mathbf{A}$	Weighted adjacency matrix of graph
$\mathbf{T}_t$	Time-evolving adjacency matrix in $[t, t + \tau)$ period
$\mathcal{T}_t^{t+l}$	Time-evolving tensor in l sequential periods
$\mathbf{w}_{f_i}$	Function set
$w_{f_{ij}}$	Word terms
$\mathbf{A}_D$	Adjacency matrix of distance graph
$\mathbf{A}_F$	Adjacency matrix of function graph
$\mathbf{A}_T$	Adjacency matrix of temporal similarity graph
$\mathbf{f}_t$	Crowd flows in $[t, t + \tau)$ period
$\mathbf{C}^{l+1}$	Dense connectivity
$\mathbf{A}_m$	Aggregation matrix of multi-graphs
G	Generative network
$\mathcal{E}_t^{t+h}$	External features in h sequential periods
$\mathbf{Z}$	Noise variable sampled from the normal distribution
$\mathcal{D}_t^{t+l}$	Average stay duration of all regions in l sequential periods
$\mathbf{d}_{i,t}^{t+l}$	Average stay duration of a region i in l sequential periods
a_i	Attention score
D	Discriminative network

FR. We divide the city into urban FR set **fr**, each FR fr_{id} has a semantic label, which represents the topic category of the FR.

**Definition 2 Multiple Graphs.** A spatio-temporal (ST) graph $\mathcal{G} = (V, E, t)$, where $V = \{v_1, v_2, ..., v_n\}$ is the set of all vertices, $|V| = n$. $(v_i, v_j) \in E$ describes the edges between vertices in $[t, t + \tau)$. $\mathbf{A} \in \mathbb{R}^{N \times N}$ is a weighted adjacency matrix which associates each edge (v_i, v_j) with its element $\mathbf{A}_{ij}$. We formulate multiple correlations in urban regions as multiple graphs, the vertices in the graph can be grids or AOIs or functional regions. $\mathbf{T}_t \in \mathbb{R}^{n*n}$ is the time-evolving adjacency matrix of the graph in $[t, t + \tau)$ period.

Definition 3 Private Car Transfer. For the snapshot in $[t, t + \tau)$ period, we formulate private car transfer between regions in as the $\mathbf{T}_t \in \mathbb{R}^{n*n}$, where n indicates the total number of regions. Specially, each $\mathbf{T}_t[i][j]$ in $\mathbf{T}_t$ represents the number of private cars transferred from region i to region j in $[t, t + \tau)$ period. We use the tensor $\mathcal{T}_t^{t+l} \in \mathbb{R}^{n*n*l}$ to indicate the private cars transfer among all n regions in l sequential periods.

Private Car Transfer Prediction. Given the l historical observations of time-evolving tensor $\mathcal{T}_{t-l}^t = \{\mathbf{T}_{t-l}, \cdots, \mathbf{T}_t\}$, predict $\mathcal{T}_{t+1}^{t+h} = \{\mathbf{T}_{t+1}, \cdots, \mathbf{T}_{t+h}\}$ in future h periods.

4 Proposed framework

As depicted in Figure 1, we present the framework for foreseeing private car transfer between urban regions. To integrate multiple spatio-temporal information, we first match the POI category to the corresponding AOI based on the spatial distance to represent the semantic information of AOIs. Second, a topic clustering algorithm is proposed to divide the city into urban FRs. Third, we employ the Spatial Joint to map the private car trips to FRs. To formulate private car transfer in FRs, we design three ST graphs. These graphs could be fed into MG-GAN to predict private car transfer in FRs. Besides, weather and date are used to produce external features if available.
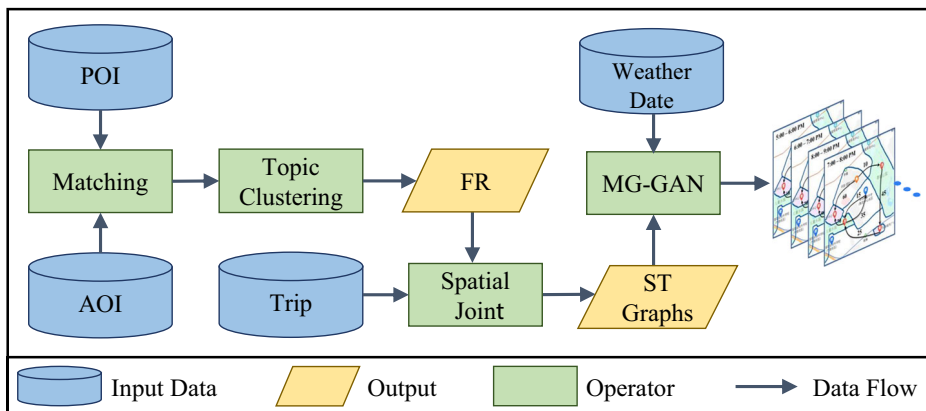
Figure 1 Framework overview

Table 2 Main functions of urban regions

Functions	Category in Amap	Code
Life Service	Shopping, Food, Daily Life	1
Park	Tourist Attraction, Pass Facilities	2
Profession	Medical Service, Governmental Organization, Finance	3
Vehicle Service	Auto Service, Auto Dealers, Auto Repair, Motorcycle Service	4
Education	Science and Educational Service	5
Enterprise	Enterprises	6
Residence	Accomodation, Commercial House	7
Transportation	Transportation Service, Place Name, Road Furniture	8
Sport	Sport and Recreation	9

4.1 Topic clustering algorithm

To identify urban functional regions, we propose a topic clustering algorithm. The inputs are the AOI set **ar** and the number of clusters m. The output is FR set **fr**. First, AOIs with similar distances will be clustered into the same sub-region by k-means++ clustering algorithm with Haversine distance [3]. Second, the latent dirichlet allocation [5] is applied for mining the topic category of each cluster. Specifically, we extract the word terms in the category label, belonging to the same function in all topics. As shown in Table 2, it is recorded as a set $\mathbf{w}_{f_i} = \left\{ w_{f_{i1}}, w_{f_{i2}}, \cdots, w_{f_{ik}} \right\}$. Then, we calculate the strength of the function of i in the FR:

$$f_i = \sum_{j=1}^{k} c \times p\left(w_{f_{ij}}\right) \times q\left(w_{f_{ij}}\right) \times w(i). \tag{1}$$

where $p\left(w_{f_{ij}}\right)$ indicates the probability that the topic of $w_{f_{ij}}$ belongs to the FR document. $q\left(w_{f_{ij}}\right)$ indicates the probability of the word term $w_{f_{ij}}$ to its topic category. c is a constant set to prevent floating-point underflow during the calculation and $w(i)$ is a weight value set for the category i. We set the FR with highest f_i to be the topic category.

4.2 Multiple graph-based GAN

In this subsection, we first model multiple correlations of private car transfer between regions as multiple ST graphs [33], including distance, function, and temporal similarity graph. Then, we predict the time-evolving adjacency matrix of the graph through the proposed MG-GAN.

4.2.1 Multiple graph modeling

We define $\mathbf{A} = \{\mathbf{A}_D, \mathbf{A}_F, \mathbf{A}_T\}$ as the adjacency matrix of graphs, where $\mathbf{A}_D, \mathbf{A}_F$, and $\mathbf{A}_T$ represent distance, function, and temporal similarity graph respectively.

a) Distance Graph. Private car users may go to the nearest region to complete activities [27]. We construct the distance graph based on the Haversine distance [14] between the

regions, and denote the adjacency matrix of the distance graph as $\mathbf{A}_D$, and each element $\mathbf{A}_{D,ij}$ in the matrix is defined as:

$$\mathbf{A}_{D,ij} = dist(v_i, v_j)^{-1} \in [0, 1], \tag{2}$$

$$\text{dist}(v_i, v_j) = 2 \times e \times \arcsin\sqrt{\varepsilon}, \tag{3}$$

$$\varepsilon = \sin^2\left(\frac{lat_i - lat_j}{2}\right) + \cos(lat_i)\cos(lat_j)\sin^2\left(\frac{lon_i - lon_j}{2}\right), \tag{4}$$

where $dist(v_i, v_j)$ denotes Haversine distance of two regions, $v_i = (lon_i, lat_i)$ and $v_j = (lon_j, lat_j)$ represent the center points of regions v_i and v_j, respectively. $e = 6371.004$ is the approximate Earth's radius.

b) Function Graph. Regions with similar functions may have strong correlations [10], and their attractiveness to private cars is also similar. We measure functional similarity between the two regions by the cosine of the two function vectors and denote the adjacency matrix of the function graph as $\mathbf{A}_F$. Each element $\mathbf{A}_{F,ij}$ in the matrix is defined as:

$$\mathbf{A}_{F,ij} = \cos(\mathbf{p}_{v_i}, \mathbf{p}_{v_j}) \in [0, 1], \tag{5}$$

where $\mathbf{p}_{vi}$ and $\mathbf{p}_{vj}$ are the AOI category vectors of regions v_i and v_j, and the dimension equal the number of AOI categories, and each entry represents the number of a specific AOI category in the region. The AOI category is illustrated in Table 2.

c) Temporal Similarity Graph. We introduce flow correlations to capture the temporal similarity between a region pair. Let $\mathbf{A}_T$ denote the flow similarity graph's adjacency matrix. We use the Pearson correlations coefficient between time-series flows of a region pair to quantify its correlations, and each element $\mathbf{A}_{T,ij}$ in the matrix can be calculated by:

$$\mathbf{A}_{T,ij} = \frac{\sum_{m=1}^{n}\left(\mathbf{fi}_m - \bar{\mathbf{N}}\right)\left(\mathbf{fj}_m - \bar{\mathbf{N}}\right)}{\sqrt{\sum_{m=1}^{n}\left(\mathbf{fi}_m - \bar{\mathbf{N}}\right)^2}\sqrt{\sum_{m=1}^{n}\left(\mathbf{fj}_m - \bar{\mathbf{N}}\right)^2}} \in [-1, 1], \tag{6}$$

wher $\mathbf{fi}$ and $\mathbf{fj}$ are time series that represent private car flows of two regions v_i and v_j, $\bar{\mathbf{fi}}$ and $\mathbf{fj}$ are the mean of $\mathbf{fi}$ and $\mathbf{fj}$.

Here we select three temporal similarity [32] to construct the graph including, hourly closeness, daily period, and weekly trend correlations, denoted as $\mathbf{A}_T = \{\mathbf{A}_{hour}, \mathbf{A}_{day}, \mathbf{A}_{week}\}$. For the current crowd flows $\mathbf{f}_t$ in $[t, t+\tau)$ period, the three historical flows in all regions can be simplified as:

– Hourly closenesss:
  $\mathbf{f}_{hour} = \{f_{t-l_r} \cdots f_{t-1}\}$,
– Daily period:
  $\mathbf{f}_{day} = \{f_{t-l_d \cdot d}, f_{t-(l_d-1)\cdot d} \cdots f_{t-d}\}$,
– Weekly trend:
  $\mathbf{f}_{week} = \{f_{t-l_w \cdot w}, f_{t-(l_w-1)\cdot d} \cdots f_{t-w}\}$,

where f_{t-l} denotes the private car flows in interval $[t-l, t-l+\tau)$. d and w are the day and week span. l_r, l_d, and l_w are the lengths of these three parts of input sequences. Substituting the $\mathbf{f}_{hour}$, $\mathbf{f}_{day}$ and $\mathbf{f}_{week}$ of all regions into Equation (6) can calculate the adjacency matrices of the temporal similarity graph.

4.2.2 Generative network

In the following, we put forward multi-graph dense convolutions with gated recurrent networks as the generative network G, and the structure is shown in Figure 2. Each sub-network
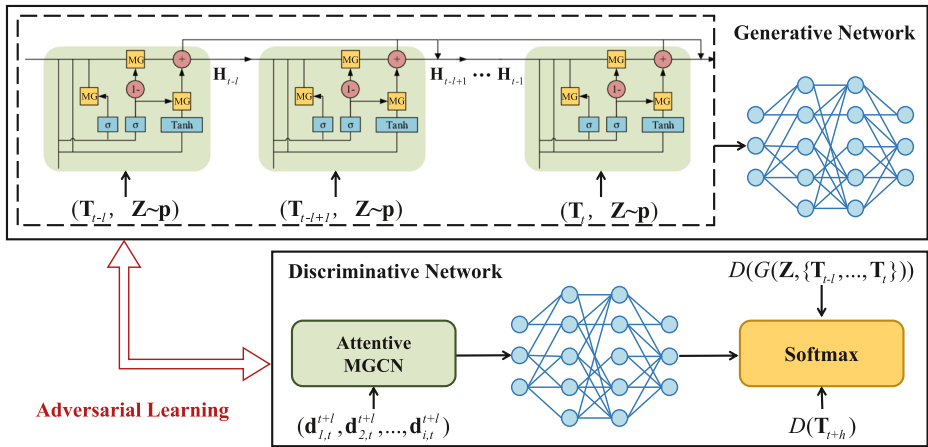
Figure 2 MG-GAN

contains a multi-graph dense graph convolution and a gated recurrent network. These multiple sub-networks are densely connected to form G through a fully connected network. The inputs of G are historical observations $\mathcal{T}_{t-l}^{t}$, multiple adjacency matrix $\mathbf{A}$, external features $\mathcal{E}_{t}^{t+h}$ in h sequential periods, and noise $\mathbf{Z}$. The external features are used for multi-step prediction since private car transfer is closely related to weather and holidays. $\mathbf{Z}$ is the noise variable sampled from the normal distribution.

We first leverage GCN [15] to transform and propagate information for the graph $\mathcal{G}$:

$$\mathbf{X}^{l+1} = \sigma\left(\tilde{\mathbf{D}}^{-1/2}\tilde{\mathbf{A}}\tilde{\mathbf{D}}^{-1/2}\mathbf{X}^l\mathbf{W}^l\right), \tag{7}$$

where $\mathbf{X}^l$, $\mathbf{X}^{l+1}$ are the correlations matrices of n regions in layer l and $l+1$, respectively. σ is the activation function $ReLU$. $\tilde{\mathbf{A}} = \mathbf{A} + \mathbf{I}_n$ is the adjacency matrix with self-connection. $\tilde{\mathbf{D}}$ is the diagonal degree matrix of $\tilde{\mathbf{A}}$. $\mathbf{W}^l$ is a learnable weighted matrix shared over all regions. To simplify notations, we summarize the operation in (7) as (8):

$$\mathbf{X}^{l+1} = f_g(\mathbf{A}, \mathbf{X}^l). \tag{8}$$

The dense graph convolutions are used to capture the global and local spatial correlations. Inspired by DenseNet, we introduce densely connected blocks in the GCN [12]. As shown in Figure 2, with densely connected blocks, the input of l layer comes from not only the correlations representation of the previous layer $\mathbf{X}^l$ but also the output from all previous layers. The l-th layer $\mathbf{X}^{l+1}$ receives the correlation-maps of all preceding layers as input:

$$\mathbf{C}^{l+1} = H_c[\mathbf{X}^0; \mathbf{X}^1; \ldots; \mathbf{X}^l], \tag{9}$$

where $H_c(\cdot)$ is a linear combination layer between multi-layer convolutional networks.

We expand the densely connected blocks to multi-graph convolutions to dedicate the multi-graph dense convolutions for modeling the global spatial correlations as follow:

$$\mathbf{X}^{l+1} = f_g(\mathbf{A}_m, \mathbf{C}^{l+1}), \tag{10}$$

$$\mathbf{A}_m = f_a(\mathbf{A}; \theta_i), \tag{11}$$

where $\cup$ denotes the sum aggregation function. $\mathbf{A}_m \in \mathbb{R}^{N \times N}$ represents the aggregation matrix of multiple graphs $\mathbf{A} \in \{\mathbf{A}_D, \mathbf{A}_F, \mathbf{A}_T\}$ parameterized by θ_i.

We embed multi-graph dense convolutions (MG in Figure 2) in gated recurrent units to capture the spatio-temporal correlations synchronously. For convenience, $\tilde{\mathbf{X}}_t[i,:]$ represents the MG, and $\tilde{\mathbf{H}}_{t-1}[i,:]$ is the hidden representations from the previous step. For each vertex v_i at time step t, the process of multi-graph dense convolutions with gated recurrent networks can be expressed as follows:

$$
\begin{aligned}
u_t &= \sigma_u \left(\mathbf{W}_u \tilde{\mathbf{X}}_t[i,:] + \mathbf{U}_u \tilde{\mathbf{H}}_{t-1}[i,:] + \mathbf{b}_u \right), \\
r_t &= \sigma_r \left(\mathbf{W}_r \tilde{\mathbf{X}}_t[i,:] + \mathbf{U}_r \tilde{\mathbf{H}}_{t-1}[i,:] + \mathbf{b}_r \right), \\
c_t &= \tanh \left(\mathbf{W_c} \tilde{\mathbf{X}}_t[i,:] + \mathbf{U_c} \left(\mathbf{r_t} \odot \mathbf{U_c} \tilde{\mathbf{H}}_{t-1}[i,:] \right) + \mathbf{b_c} \right), \\
\mathbf{H}_t[i,:] &= (1 - u_t) \tilde{\mathbf{H}}_{t-1}[i,:] + u_t \odot c_t,
\end{aligned}
\tag{12}
$$

where $\tilde{\mathbf{X}}_t[i,:]$, $\mathbf{H}_t[i,:]$ are the input and output at time step t, respectively. $\odot$ denotes the element-wise multiplication.

We utilize the simplified notation to represent the G (with noise $\mathbf{Z}$ and historical sequence $\mathcal{T}_{t-l}^t$ as the input):

$$
\tilde{\mathcal{T}}_{t+1}^{t+h} = G \left(\mathbf{Z}, \mathcal{T}_{t-l}^t, \mathcal{E}_{t+1}^{t+h} \right)
\tag{13}
$$

4.2.3 Discriminative network

The longer duration private car stays in a region, the more attractive this region is [20]. When the number of private cars transferred to a region is larger, the stay duration in the region will be longer. At the same time, the region's attractiveness has increased, thereby attracting more private cars. Inspired by this, we develop a discriminative network D to discriminate the prediction results of private car transfer obtained by the generation network G. The iterative adversarial processes between generating network and discriminating network enhance the MG-GAN's ability. We first take the average stay duration of private cars in each region as the weight of regional importance. Then, we propose an attentive MGCN based on the private cars' staying duration, assign different weights to different vertices nearby to learn the importance.

For node v_i, we first organize this input $\mathbf{H}_i$ according to the sequential order. Then, the average stay duration of urban regions, parameterized by a weight vector $\mathcal{D}_t^{t+l}$. Specifically, each $\mathbf{d}_{i,t}^{t+l}$ in $\mathcal{D}_t^{t+l}$ represents the average staying time of a region i in the previous T times. The attention is formulated as:

$$
\begin{aligned}
e_i &= \left(\mathcal{D}_t^{t+l} \mathbf{H}_i \right)^{\mathrm{T}} \boldsymbol{u}, \\
a_i &= \mathrm{SoftMax}\,(e_i) = \frac{\exp(e_i)}{\sum_{l=1}^k \exp(e_i)},
\end{aligned}
\tag{14}
$$

where $\boldsymbol{u}$ is a weight vector, which is initialized as a random vector and jointly learned during the training process.

After obtaining the attention coefficient, we calculate the linear combination represented for each vertex and generate the output of the attention layer, which can be denoted as $\mathbf{H}_{out}^i \in \mathbb{R}^{T \times d}$.

$$
\mathbf{H}_{out}^i = \sum_{l=1}^k a_i \mathbf{H}_i,
\tag{15}
$$

In adversarial training of MG-GAN, we use the discriminative network D as a reward function to further enhance the performance of the G by updating the D and the G alternately and iteratively. D consists of an attentive multi-graph convolution network (MGCN)

and a fully connected network. D alternatively takes G's output $\mathcal{T}_{t+1}^{t+h}$ or the ground truth $\tilde{\mathcal{T}}_{t+1}^{t+h}$ as the input. The details of the D can be formulated as follow:

$$D\left(\mathcal{T}'\right) = \left(\sigma\left(\alpha'\mathbf{W}_h^D + \mathbf{b}_h^D\right)\mathbf{W}_o^D + \mathbf{b}_o^D\right), \tag{16}$$

where $\mathcal{T}' \in \{\tilde{\mathcal{T}}_{t+1}^{t+h}, \mathcal{T}_{t+1}^{t+h}\}$ with α' as the reshaped row-wise long vector. $\{\mathbf{W}_h^D, \mathbf{b}_h^D\}$ and $\{\mathbf{W}_o^D, \mathbf{o}_h^D\}$ are respectively the parameters of the hidden layer and the output layer; $\sigma(\cdot)$ represents the sigmoid activation function of the hidden layer.

4.2.4 Loss function

We introduce a pre-training process for G with the following loss function:

$$\begin{aligned}&\min_{\theta_G} h_G\left(\theta_G; \mathbf{Z}, \mathcal{T}_{t-l}^t, \mathbf{T}_t\right) = \\&\left\|\mathbf{T}_t - G\left(\mathbf{Z}, \mathcal{T}_{t-l}^t\right)\right\|_F^2 + \frac{\lambda}{2}\|\theta_G\|_2^2,\end{aligned} \tag{17}$$

where θ_G represents the parameters of G and λ is the parameter to control the effect of the L_2-regularization term. G tries to reconstruct the current matrix given by the observations $\mathbf{T}_t$ and noise $\mathbf{Z}$. Such a process can help G fully capture the graph's latest temporal information, which is considered the most similar features to the ground truth $\mathcal{T}_{t+1}^{t+h}$.

We utilize the gradient descent method to update D's parameters (notated as θ_D) with G's parameters fixed via the following loss function:

$$\begin{aligned}&\min_{\theta_D} h_D\left(\theta_D; \mathbf{Z}, \mathcal{T}_{t-l}^t, \mathbf{T}_t\right) = \\&\mathrm{E}\left[D\left(\mathbf{T}_t\right)\right] - \mathrm{E}\left[D\left(G\left(\mathbf{Z}, \mathcal{T}_{t-l}^t\right)\right)\right].\end{aligned} \tag{18}$$

The Adam algorithm is used to update the parameters alternatively θ_D and θ_G until the MG-GAN converges.

5 Experiments

In this study, we use the private car and taxi trip datasets. To demonstrate the superiority of the proposed method, we select seven baselines. In addition, we consider the Mean Square Error (MSE) and the Kullback-Leibler divergence (KL) to evaluate the performance of MG-GAN.

5.1 Datasets

Private car trip data We use the private car trip dataset, as illustrated in Table 3. The dataset was collected from real-world urban environments using vehicle positioning techniques [19]. We choose an administrative district of Changsha and Shenzhen, respectively, as shown in Figure 3.[1] This dataset includes fields: id, start and stop time, longitude, latitude, and position. The private car trip dataset is publicly available under the consensus on research purpose only.

Taxi trip data We use another open-source dataset to evaluate the performance of all models. This dataset contains green taxi trips in NYC[2] in November 2019. We choose fields: id,

---

[1] https://github.com/HunanUniversityZhuXiao/PrivateCarTrajectoryData
[2] https://www1.nyc.gov/site/tlc/about/tlc-trip-record-data.page

Table 3 Private car trip datasets in Changsha and Shenzhen

Cities	Changsha	Shenzhen
Latitude	27.92-28.21	22.51-22.83
Longitude	112.97-113.18	113.75-113.99
Private car trips	6,267,371	17,423,606
AOIs	1407	3995
Functional regions	109	210
Grids	13 × 17	16 × 22
Timespan	2018/6/1-2018/9/30	
Holidays	6	
Weekdays	32	
Weather categories	5	

pick-up and drop-off times, locations, and location id. We set each location (taxi zone) as the graph's vertex, and the total number of locations is 265.

Multi-source data The multi-source datasets include POI, AOI, weather, as summarized in Table 3.

(a)   (b)
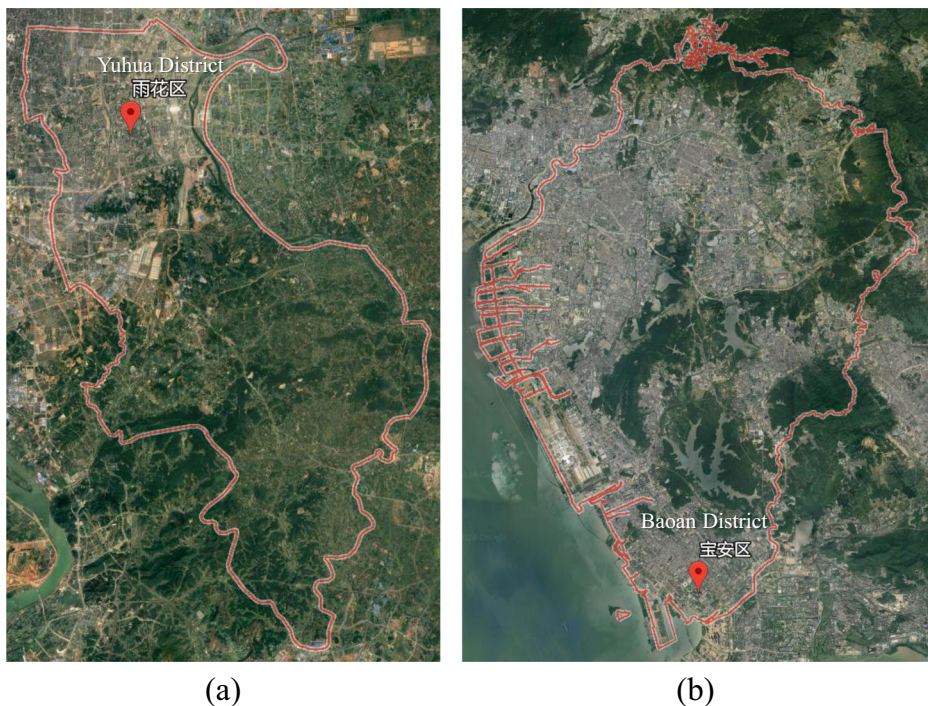
Figure 3 Visualization of administrative district boundaries. **a** Yuhua District, Changsha. **b** Baoan District, Shenzhen

5.2 Baselines

We compare our proposed model with several baselines as follows.

– **HA.** Historical average (HA) uses the historical average transfer flows between regions in the historical periods as the prediction. We choose the first 70% as the training set of the HA model, 10% as the validation set, and the remaining 20% as the test set.

– **BO-SVR.** Support vector regression based on Bayesian optimization (BO-SVR) is a non-linear time series prediction method [28]. We set three tuning parameters $(C; \varepsilon; \sigma)$ as $(1; 0.1; 1)$.

– **ConvLSTM.** Convolutional Long-Short Term Neural Network (ConvLSTM) variates LSTM containing a convolution operation inside the LSTM cell [26]. Both the models are special RNN capable of learning long-term dependencies. We implement the ConvLSTM model with TensorFlow. We set the convolution filter size to $3 * 3$, and the number of convolution kernels to 8. The LSTM unit is set to 5.

– **3D CNN.** 3D Convolution Neural Network (3D CNN) in the convolution stages of CNNs compute features from both spatial and temporal dimensions [24]. We implement the ConvLSTM model with TensorFlow. We set the convolution filter size to $3 * 3 * 1$, $1 * 3 * 3$, and $3 * 3 * 3$. We set six layers and the number of convolution kernels to 16.

– **DeepSTN+.** Deep learning-based spatial-temporal network plus (DeepSTN+) modeling long-range dependence and semantic effects for crowd flow prediction in metropolis [18]. We set the number of ResPlus units to 2.

– **STDN.** Spatial-Temporal Dynamic Network (STDN) is a unified traffic prediction framework in which a flow gating mechanism is introduced to learn the spatial features, and a periodically shifted attention mechanism is designed to learn temporal features [31]. The convolution kernel size is set to 3.

– **GCN-GAN.** Graph Convolution Network is a non-linear model to tackle the temporal link prediction task of weighted dynamic networks [16]. The window size of the history network snapshot to be considered is 10.

5.3 Settings and metrics

In the preprocessing step, we divide the urban region in three parallel ways, as shown in Definition 1. Thus, the multiple ST graphs have three vertices, as depicted in Figure 4, which are grids, AOIs, or FRs. We divide the ratio of training, validation, and test sets to

(a)	(b)	(c)
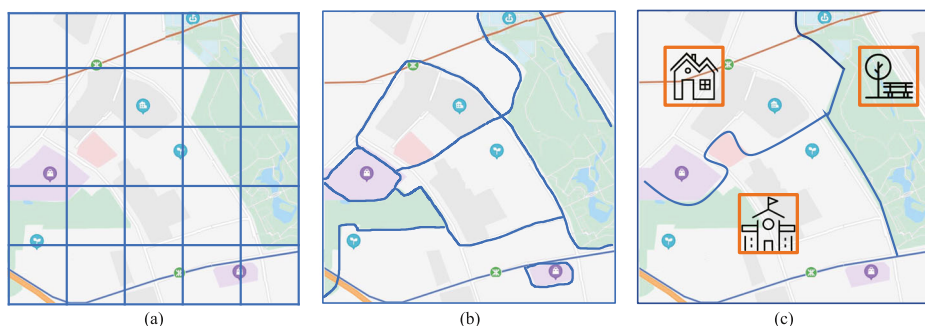
Figure 4 Examples of regions types. **a** Grid. Divid the city into 5×5 equal-sized grids. **b** AOI. 9 AOIs. **c** Functional Region. 3 categories of FRs: (1) Residence. (2) Park. (3) Education

7:2:1. The time slice $\tau = 1$ h, dividing the day into 24 equal-length slices. The MG-GAN is implemented on two Tesla V100 GPUs. In addition, Python 3.6, Tensorflow 1.9.0, and Cuda 11.1 are involved in helping build deep graph neural networks. The training stage is performed using the Adam optimizer and the batch size is 32. We set the EarlyStopping strategy. If the performance does not improve, the training process will be terminated. The initial learning rate $lr = 0.0015$ dropped to 10% every 1000 iterations, the drop rate $d = 0.5$. The L_2-regularization term λ is set to 1e-5. In the prediction stage, we select the input sequence length from the range of $\{1, 2, 3, 4, 5\}, \{1, 2, 3, 4, 5\}, \{1, 2, 3, 4\}$ which respectively corresponds to three different temporal correlations (hour, day, and week). We stack three feedforward layers in the final prediction stage.

To evaluate the prediction performance of MG-GAN and baselines, we employ two standard metrics: mean squared error (MSE) and Kullback-Leibler divergence (KL):

$$MSE = \left\| \mathcal{T}_{t+h} - \tilde{\mathcal{T}}_{t+h} \right\|_F^2 / (n \times n), \tag{19}$$

$$KL(\mathbf{P}\|\mathbf{Q}) = \sum_{i,j=1}^{N} f\left(\mathbf{P}_{ij}, \mathbf{Q}_{ij}\right), \tag{20}$$

$$\mathbf{P}_{ij} = \frac{(\mathcal{T}_{t+h})_{ij}}{\sum_{ij=1}^{N} (\mathcal{T}_{t+h})_{ij}}, \mathbf{Q}_{ij} = \frac{(\mathcal{T}_{t+h})_{ij}}{\sum_{ij=1}^{N} (\mathcal{T}_{t+h})_{ij}}. \tag{21}$$

5.4 Results and discussions

Urban functional regions identification We pick the silhouette coefficient as the topic clustering algorithm metric and calculate the k value with the smallest SC as the total number of regions. Then, we average the silhouette coefficients of all points to present the clustering's total silhouette coefficient. To show the uniformity of the clustering results, we visualize the center points of all FRs. Figure 5a depicts the 109 center points in Yuhua District, Changsha, which means $k = 109$ is the best hyperparameter for this city's region division. Figure 5b depicts the 210 center points in Baoan district, Shenzhen. The center point's color corresponds to Table 2, and different colors represent different functions of urban regions.

Hyperparameter sensitivity We choose the relevant hyperparameters of the MG-GAN. Different numbers of hidden units may substantially affect the prediction performance. We experiment with the different hidden units and select the optimal value by comparing the

(a) Yuhua District, Changsha   (b) Baoan District, Shenzhen
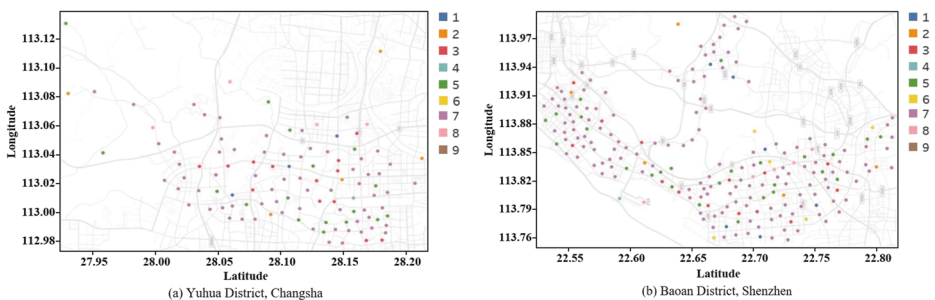
Figure 5 Visualization of the central points of FRs in Changsha and Shenzhen
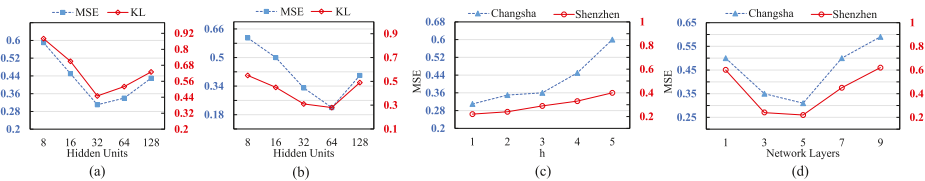
Figure 6 Hyperparameter sensitivity. **a** Error on city Changsha. **b** Error on city Shenzhen. **c** Prediction time step h. **d** Network Layers

prediction results. Figure 6a and b depict the MSE for different hidden units in the city of Changsha and Shenzhen, respectively. The error is the smallest when the number is 32 in Changsha. When the number of hidden units is 64 in Shenzhen, the prediction error is the lowest. When increasing the number of hidden units, the prediction error firstly decreases and then increases. The possible reason is that when the number of hidden units is larger than a certain degree, the model complexity and the computational difficulty increase. In Figure 6c, we set T from one to six. The MSE increases as T increases, this makes sense since the temporal correlations between observed and future transfer flow become lower when T goes large. Figure 6d depicts the layers of multi-graph dense convolutions with gated recurrent networks, and the optimal number of layers is five.

Overall performance For the above urban regions, we predict private car transfer in different periods. Table 4 presents the average results for all the models in three cities based on the best hyperparameters in Figure 6. All models' evaluation results confirm that FR is the best vertex type, followed by AOI and the grid. The reason is that FRs have rich semantic information, and more importantly, they can alleviate the imbalance and sparsity of the original data.

Compared to the selected baselines, MG-GAN achieves superior performance, followed by GCN-GAN, STDN, and DeepST+. Traditional models such as HA and BO-SVR fail to perform well since the spatio-temporal correlations are hard to capture. Also, 3D CNN and ConvLSTM fail to capture the non-Euclidean correlations between the regions. The effect of 3D CNN is better since it captures spatio-temporal correlations simultaneously.

Table 4 Evaluations on private car and taxi trip dataset

Cities	Changsha						Shenzhen						NYC	
Vertices	Grid		AOI		FR		Grid		AOI		FR		Location	
Metrics	MSE	KL	MSE	KL	MSE	KL	MSE	KL	MSE	KL	MSE	KL	MSE	KL
HA	5.79	6.38	5.35	5.98	5.10	5.66	4.69	5.08	4.22	4.81	4.08	4.37	8.68	9.96
BO-SVR	4.86	3.49	2.51	2.64	1.68	1.76	3.42	2.46	1.77	1.86	1.18	1.24	3.68	5.18
ConvLSTM	2.35	1.69	1.21	1.41	0.81	0.94	1.65	1.19	0.86	0.99	0.57	0.66	1.57	1.68
3D CNN	1.45	1.64	0.81	0.85	0.55	0.73	0.98	1.66	0.75	0.82	0.45	0.42	0.98	1.367
DeepST+	1.44	1.04	0.75	1.34	0.50	0.89	1.01	0.73	0.53	0.95	0.35	0.63	1.27	1.84
STDN	1.15	0.83	0.58	0.89	0.38	0.60	0.81	0.58	0.42	0.63	0.28	0.42	0.98	0.91
GCN-GAN	1.04	1.16	0.50	0.61	0.37	0.68	0.71	1.13	0.53	0.77	0.27	0.38	0.87	1.17
MG-GAN	0.85	0.61	0.43	0.41	0.32	0.28	0.60	0.43	0.31	0.24	0.23	0.22	0.69	0.63

Table 5 Ablation analysis

Model	Changsha		Shenzhen	
	MSE	KL	MSE	KL
MG-GAN w/o F	0.48	0.62	0.35	0.43
MG-GAN w/o T	0.53	0.67	0.41	0.51
MG-GAN w/o D	0.38	0.49	0.29	0.47
MG-GAN w/o E	0.33	0.47	0.25	0.45
MG-GAN	0.31	0.45	0.22	0.28

Although STDN and DeepST+ incorporate rich semantic and external features into their models, we cannot apply multi-graph modeling since they are pixel-level modeling. GCN-GAN ignores multiple correlations between regions and lacks the impact of external factors. For NYC, we do not divide it into FRs. Thus, its prediction error is largest than the other two cities. Finally, the results in Shenzhen are better than those in Changsha. The reason is that more private car trips in Shenzhen than that used in Changsha, and it can extract the spatio-temporal correlations of private car transfer more comprehensively.

Ablation study In the optimal hyperparameter settings, we evaluate the following variants of MG-GAN by removing different components from the model: (1) Function graph (F), (2) Temporal similarity graph (T), (3) Distance graph (D), (4) External component (E). As illustrated in Table 5, removing any component causes an error increase, which justifies each component's importance. The results demonstrate that removing the temporal similarity graph has the greatest impact on the model. The reason is that the temporal similarity graph models the relationship between regions from the different perspectives of historical flow similarity. Function graph also plays a significant role due to the ability to use urban regions' semantic information fully. Followed by the distance graph. The least impact is the external component. The possible reason is that external features' influence is smaller than that of the spatio-temporal correlations of private car transfer.

Efficiency comparison Under the optimal hyperparameter settings, we compare the running time of the proposed approach on different datasets, as shown in Table 6. The unit of the running time in seconds. In the preprocessing stage, the NYC dataset has the shortest

Table 6 Results of efficiency comparison

| Dataset	Stage	Time (s)
	preprocessing	3.0248
Changsha	training	1.5966
	predicting	0.0052
	preprocessing	5.5165
Shenzhen	training	2.3856
	predicting	0.0078
	preprocessing	0.0529
NYC	training	3.1553
	predicting	0.0081

Table 7 An example of functional regions and sub-regions in Yuhua District, Changsha

Functional region	Sub-region ID*	Sub-region Name	Area
Profession	B02DB06945	Changsha Central Hospital	78191
Park	B02DB027D2	Hunan Forest Botanical Garden	980384
Life service	B0FFF6LNFH	Teskin Town Square	104210
Transportation	B02DB07MDA	Changshanan Railway Station	292157
Residence	B02DB06IWB	Vanke Golden Home	7013
	B0FFGMJ9V0	Tongcheng Logistics Community	4571
Education	B02DB07MJL	Changsha Social Work College	532520
	B0FFFYFXC4	Mingde Yuhua Experimental Middle School	33217
	B0FFFDKNCE	Maple Shandong Nanhai Primary School	11292

*Unique ID in Amap

running time since the dataset has regional labels, which saves the running time of identifying FRs. In the training stage, the Changsha dataset has the shortest running time since the number of vertices in its spatio-temporal graph is the smallest. Finally, in the prediction stage, the running time of the three data sets has little difference, and all can achieve real-time prediction.
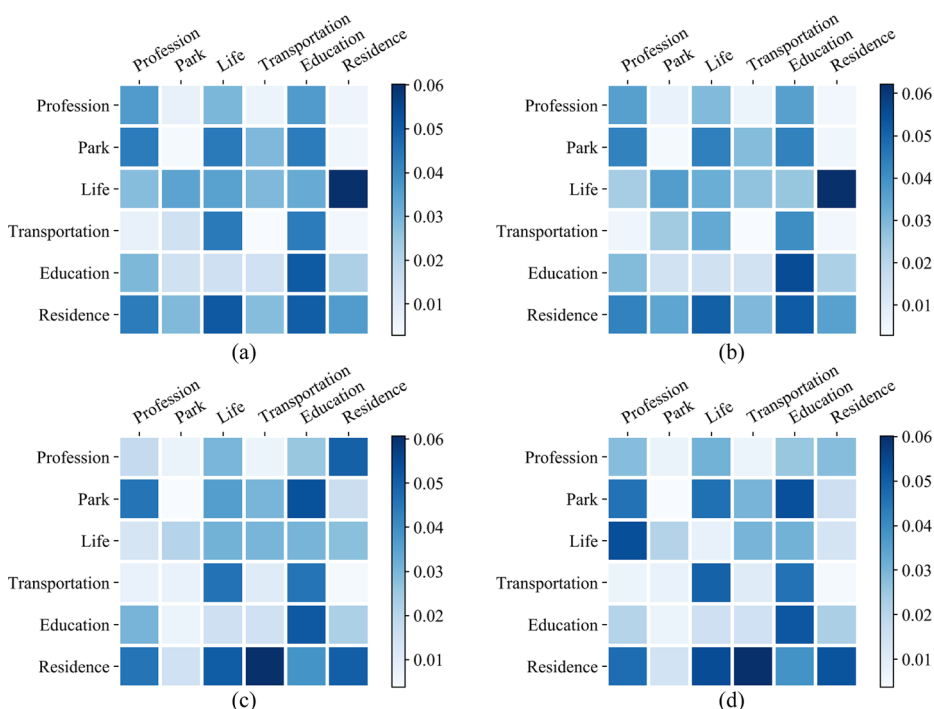
Figure 7 Predicted time-evolving adjacency matrix and ground truth in Yuhua District, Changsh, September 25, 2018. (**a**) and (**b**) are predicted adjacency matrix and ground truth from 4:00:00 to 4:59:59 pm. (**c**) and (**d**) are matrixes from 5:00:00 to 5:59:59 pm

Case study We randomly select six FRs in the south of Yuhua District, Changsha, as examples to visualize the private car transfer between them. The unique ID, name, and area of the sub-regions are shown in Table 7. For example, the residence region consists of two sub-regions that are close together. Similarly, the education region is composed of three sub-regions. We choose two consecutive periods of predicted results to show the performance of MG-GAN. The predicted time-evolving adjacency matrix and ground truth are shown in Figure 7, all the values in the adjacency matrix add up to 1. Overall, our predicted time-evolving adjacency matrices are close to the ground truth.

6 Conclusion

In this paper, we make the first attempt to foresee private car transfer between urban regions from a multi-source data perspective. We model private cars' travel in urban regions as multiple spatio-temporal graph. Then, we propose multiple graph-based generative adversarial networks called MG-GAN to predict private car transfer. Experiments on two real-world private car trip datasets demonstrate that our MG-GAN can achieve consistently better performance on region-level transfer prediction. We could infer which regions are sparse through transfer flow prediction. It is substantial for urban planners to set up infrastructure in sparse regions, thereby dispersing the transfer traffic in other regions. For example, establishing schools or large shopping malls in sparse regions, on the one hand, alleviates traffic congestion in other regions, and on the other hand, can promote economic development in these sparse regions. Our work can be applied to predict other vehicles' travel time, speed distribution, and crowd flow, especially in scenarios where imbalanced and sparse records are generated. Besides, our open-source private car trip dataset provides novel perspectives for trajectory big data mining and intelligent transportation systems. The development of real online models based on deep learning is one of our future work to timely and efficiently alert the abnormal transfer flows.

References

1. Alexander, L., Jiang, S., Murga, M., González, M.C.: Origin-destination trips by purpose and time of day inferred from mobile phone data. Transp Res Part C: Emerg Technol **58**, 240–250 (2015)
2. Alfeo, A.L., Cimino, M.G., Egidi, S., Lepri, B., Vaglini, G.: A stigmergy-based analysis of city hotspots to discover trends and anomalies in urban transportation usage. IEEE Trans Intell Transp Syst **19**(7), 2258–2267 (2018)
3. Arthur, D., Vassilvitskii, S.: k-means++: the advantages of careful seeding. In: ACM SIAM, New Orleans, Louisiana, USA, pp 1027–1035. Stanford (2007)
4. Bartle, C., Chatterjee, K.: Employer perceptions of the business benefits of sustainable transport: a case study of peri-urban employment areas in south west england. Transp Res A Policy Pract **126**, 297–313 (2019)
5. Blei, D.M., Ng, A.Y., Jordan, M.I.: Latent Dirichlet allocation. J Mach Learn Res **3**, 993–1022 (2003)
6. Chai, D., Wang, L., Yang, Q.: Bike flow prediction with multi-graph convolutional networks. In: ACM SIGSPATIAL, pp 397–400 (2018)
7. Cheung, M., Shi, J., Wright, O., Jiang, L.Y., Liu, X., Moura, J.M.: Graph signal processing and deep learning: convolution, pooling, and topology. IEEE Signal Process Mag **37**(6), 139–149 (2020)

8. Chu, K.F., Lam, A.Y., Li, V.O.: Deep multi-scale convolutional lstm network for travel demand and origin-destination predictions. IEEE Trans Intell Transp Syst **21**(8), 3219–3232 (2020)

9. Geng, X., Li, Y., Wang, L., Zhang, L., Yang, Q., Ye, J., Liu, Y.: Spatiotemporal multi-graph convolution network for ride-hailing demand forecasting. In: AAAI, vol 33, pp 3656–3663 (2019)

10. Gong, Y., Li, Z., Zhang, J., Liu, W., Zheng, Y.: Online spatio-temporal crowd flow distribution prediction for complex metro system. IEEE Trans Knowl Data Eng, pp 1–16 (2020)

11. Hu, J., Yang, B., Guo, C., Jensen, C.S., Xiong, H.: Stochastic origin-destination matrix forecasting using dual-stage graph convolutional, recurrent neural networks. In: IEEE ICDE, pp 1417–1428 (2020)

12. Huang, G., Liu, Z., Van Der Maaten, L., Weinberger, K.Q.: Densely connected convolutional networks. In: CVPR, pp 2261–2269 (2017)

13. Huang, Y., Xiao, Z., Wang, D., Jiang, H., Wu, D.: Exploring individual travel patterns across private car trajectory data

14. Inman, J.: Navigation and nautical astronomy, for the Use of British Seamen. F. & J Rivington (1849)

15. Kipf, T.N., Welling, M.: Semi-supervised classification with graph convolutional networks. ICLR, pp 1–14 (2017)

16. Lei, K., Qin, M., Bai, B., Zhang, G., Yang, M.: Gcn-gan: a non-linear temporal link prediction model for weighted dynamic networks. In: IEEE INFOCOM. Paris, pp 388–396 (2019)

17. Li, Y., Fu, K., Wang, Z., Shahabi, C., Ye, J., Liu, Y.: Multi-task representation learning for travel time estimation. In: ACM SIGKDD, pp 1695–1704 (2018)

18. Lin, Z., Feng, J., Lu, Z., Li, Y., Jin, D.: Deepstn+: context-aware spatial-temporal neural network for crowd flow prediction in metropolis. In: AAAI. Honolulu, pp 1020–1027 (2019)

19. Liu, C., Cai, J., Wang, D., Tang, J., Wang, L., Chen, H., Xiao, Z.: Understanding the regular travel behavior of private vehicles: An empirical evaluation and a semi-supervised model. IEEE Sensors J **21**(17), 19078–19090 (2021)

20. Liu, C., Wang, D., Chen, H., Li, R.: Study of forecasting urban private car volumes based on multi-source heterogeneous data fusion. J Commun **42**(3), 54–65 (2021). https://doi.org/10.11959/j.issn.1000-436x.2021018

21. Liu, W., Lai, H., Wang, J., Ke, G., Yang, W., Yin, J.: Mix geographical information into local collaborative ranking for poi recommendation. World Wide Web **23**(1), 131–152 (2020)

22. Moreira-Matias, L., Gama, J., Ferreira, M., Mendes-Moreira, J., Damas, L.: Time-evolving od matrix estimation using high-speed gps data streams. Expert Syst Appl **44**, 275–288 (2016)

23. Nasab, M.R., Shafahi, Y.: Estimation of origin-destination matrices using link counts and partial path data. Transportation **47**(6), 2923–2950 (2020)

24. Shen, B., Liang, X., Ouyang, Y., Liu, M., Zheng, W., Carley, K.M.: Stepdeep: a novel spatial-temporal mobility event prediction framework based on deep neural network. In: ACM SIGKDD. London, pp 724–733 (2018)

25. Shi, H., Yao, Q., Guo, Q., Li, Y., Zhang, L., Ye, J., Li, Y., Liu, Y.: Predicting origin-destination flow via multi-perspective graph convolutional network. In: IEEE ICDE, pp 1818–1821 (2020)

26. Shi, X., Chen, Z., Wang, H., Yeung, D.Y., Wong, W.K., Woo, W.C.: Convolutional lstm network: a machine learning approach for precipitation nowcasting. Adv Neural Inform Process Syst **2015**, 802–810 (2015)

27. Simini, F., González, M.C., Maritan, A., Barabási, A.L.: A universal model for mobility and migration patterns. Nature **484**(7392), 96–100 (2012)

28. Wang, D., Wang, C., Xiao, J., Xiao, Z., Chen, W., Havyarimana, V.: Bayesian optimization of support vector machine for regression prediction of short-term traffic flow. Intell Data Anal **23**(2), 481–497 (2019)

29. Wang, Y., Yin, H., Chen, H., Wo, T., Xu, J., Zheng, K.: Origin-destination matrix prediction via graph convolution: a new perspective of passenger demand modeling. In: ACM SIGKDD, pp 1227–1235 (2019)

30. Yang, M., Liu, J., Chen, L., Zhao, Z., Chen, X., Shen, Y.: An advanced deep generative framework for temporal link prediction in dynamic networks. IEEE Trans Cybern **50**(12), 4946–4957 (2019)

31. Yao, H., Tang, X., Wei, H., Zheng, G., Li, Z.: Revisiting spatial-temporal similarity: a deep learning framework for traffic prediction. In: AAAI. Honolulu, pp 5668–5675 (2019)

32. Zhang, J., Zheng, Y., Sun, J., Qi, D.: Flow prediction in spatio-temporal networks based on multitask deep learning. IEEE Trans Knowl Data Eng **32**(3), 468–478 (2019)

33. Zhang, M., Li, T., Li, Y., Hui, P.: Multi-view joint graph representation learning for urban region embedding. In: IJCAI. Yokohama, pp 4431–4437 (2021)

34. Zhang, Y., Wang, S., Chen, B., Cao, J., Huang, Z.: Trafficgan: network-scale deep traffic prediction with generative adversarial nets. IEEE Trans Intell Transp Syst **22**(1), 219–230 (2021)

35. Zheng, L., Xia, D., Chen, L., Sun, D.: Understanding citywide resident mobility using big data of electronic registration identification of vehicles. IEEE Trans Intell Trans Syst 4363–4377 (2019)

Publisher's note Springer Nature remains neutral with regard to jurisdictional claims in published maps and institutional affiliations.

Affiliations

Chenxi Liu[1] (ID) **· Zhu Xiao[1] · Dong Wang[1] · Minhao Cheng[2] · Hongyang Chen[3] · Jiawei Cai[1]**

✉ Dong Wang
   wangd@hnu.edu.cn

✉ Hongyang Chen
   dr.h.chen@ieee.org

   Chenxi Liu
   cxliu@hnu.edu.cn

   Minhao Cheng
   mhcheng@cs.ucla.edu

   Jiawei Cai
   caijw@hnu.edu.cn

[1] College of Computer Science and Electronic Engineering, Hunan University, Changsha, China
[2] Department of Computer Science, University of California Los Angeles, Los Angeles, CA, USA
[3] Intelligent Computing Platform Research Center, Zhejiang Lab, Hangzhou, China